

# Receptor-Mediated and Intrinsic Polarization and Their Interaction in Chemotaxing Cells

J. Krishnan\* and P. A. Iglesias†

\*Chemical Engineering and Chemical Technology, Imperial College, London, United Kingdom; and †Electrical and Computer Engineering, Johns Hopkins University, Baltimore, Maryland

**ABSTRACT** Polarization—the clear and persistent localization of different signaling molecules to opposite ends of the cell—is critical for effective chemotaxis in eukaryotic systems. In many systems, polarization can also occur without an externally imposed chemical gradient. We build a modeling framework to study the relationship between the intrinsic capacity for polarization, and that induced by an external gradient. Working within this framework, we analyze different scenarios for the interaction of these pathways. The models are qualitatively simplified, motivated by known properties of the signaling pathways. We also examine the possible role of nonlinear transitions occurring in the polarization pathways. The modeling framework generates testable predictions regarding the relationship between intrinsic polarization and that induced during chemotaxis, and is the first step toward a systematic analysis of the interaction between these pathways.

## INTRODUCTION

There is much interest in achieving a quantitative understanding of the underlying signal transduction networks that regulate biological processes, an area referred to as “Systems Biology.” Eukaryotic chemotaxis—the directed migration of eukaryotic cells in response to gradients of external chemicals—is an excellent candidate for such a detailed theoretical and experimental study for various reasons. First, it incorporates basic biological elements such as motility and the sensing and response to external signals. Second, it is implicated in many physiological processes including wound healing, tumor metastasis, and development.

Experimentally, single-cell chemotaxis is studied in a diverse number of cells (1–3). Because chemotaxis is a complex process, many experimental and modeling efforts have focused on the first stage of this process, known as gradient sensing: the process by which cells convert information about the chemical concentration of their surroundings into an internal signal to guide their motion (4–10). In many systems, the gradient sensing process is functional in cells where the actin cytoskeleton has been impaired (2,11,12). Valuable insights into gradient sensing have been obtained by modeling the process in this simpler setting (13,14). Other phenomenological efforts focus on the description of random motility, biased random walk and persistent chemotaxis (15).

Additional features need to be understood to make a transition from gradient sensing to chemotaxis and cell migration, including a detailed study of the interaction of gradient sensing with the actin cytoskeleton leading to motility. Here, we focus on a crucial feature of chemotaxing cells: polarity. Though it has long been recognized that cell polarity is of critical importance in migration (16), there are few system-

atic experimental or theoretical studies of cell polarity in this context. In fact, the term “cell polarity” is used to mean somewhat different things by different researchers. We understand cell polarity to be the localization of various signaling components to opposite ends of the cell in a persistent fashion, with any attendant morphological change (4,5). This definition of polarity is appropriate for our purpose, because the formation of a *persistent* front and back is of vital importance for efficient chemotaxis. Polarity as a phenomenon, that is, the establishment of an axis, is a topic that cuts across many biological processes, and is of relevance in development, cell growth and division besides cell migration (17,18).

In chemotaxing cells, polarization occurs at a timescale of one to a few minutes after exposure to an external chemoattractant gradient. However, cells can also become polarized without an externally imposed gradient (19,20). For instance, neutrophils polarize (in an apparently random direction) when stimulated by a spatially homogeneous dose of chemoattractant. *Dictyostelium* cells become highly polarized in the course of their development (5). Thus, in these systems, there is an intrinsic capability for polarization that does not need an externally imposed gradient. Different assumptions regarding how this intrinsic polarization may be exploited for chemotaxis have been made, either explicitly or implicitly (9,21).

There are many questions regarding this polarization process: how does it come about in the absence of externally imposed chemical gradients? How, if at all, does the cell exploit this capability to polarize, when subject to a chemical gradient? What are the factors that control the intrinsic cell polarity and how do receptor signals interact with them? Are there any differences in the timescales of these processes? What are the roles of nonlinear dynamic phenomena and self-organization in these processes?

Here, we develop a modeling framework to address various aspects of the polarization process, including the

Submitted April 17, 2006, and accepted for publication October 12, 2006.

Address reprint requests to P. A. Iglesias, Tel.: 410-516-6026; E-mail: pi@jhu.edu.

© 2007 by the Biophysical Society

0006-3495/07/02/816/15 \$2.00

doi: 10.1529/biophysj.106.087353

interaction between intrinsic polarization, such as the one induced during development in *Dictyostelium* cells, and that driven by an externally applied chemoattractant gradient. We employ simplified models, motivated by experimental data on various pathways involved in gradient sensing and motility. We study the implications of various scenarios regarding the interaction. This analysis provides us with insight into how external signals and intrinsic processes may interact, and makes various testable predictions that do not require full knowledge of the biochemical entities involved. It also brings into focus the possible role of nonlinear dynamic transitions in the polarization process.

## The modeling framework

We develop a modeling framework to investigate the relationship between intrinsic and externally induced polarity; see Fig. 1 A. We consider several possibilities for the underlying mechanisms in a way that suggests experiments that can distinguish between them, thus enabling us to study polarity from a systematic perspective and focus on several key questions.

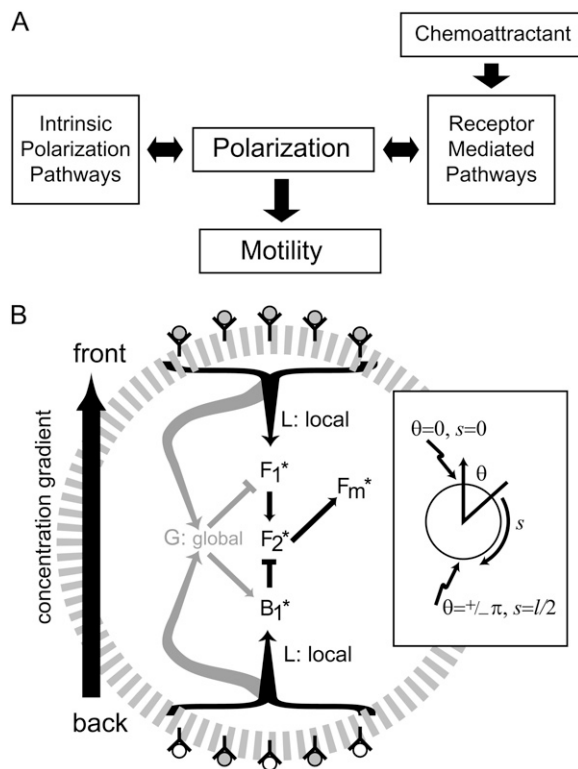


**FIGURE 1** Schematic of cell and receptor-mediated pathways in the simplified models. (A) We assume that cell polarization is dictated by a combination of intrinsic and receptor-mediated pathways. (B) Receptor-mediated signaling involves both local and global pathways, and regulates  $F_1^*$  and  $B_1^*$ . These species regulate  $F_2^*$ , which controls the motility element  $F_m^*$ . In a gradient,  $F_1^*$  and  $B_1^*$  play dual roles in leading to a greater  $F_2^*$  at the leading edge. An intrinsic pathway (not shown) regulates the frontness and backness components (see text). The inset shows the definition of the spatial parameter used in the simulations.

A polarized chemotaxing *Dictyostelium* cell has different components localized near either end. For instance, PI3K, PI(3,4,5)P<sub>3</sub>, PI(3,4)P<sub>2</sub>, F-actin, PAK1, and Rac are found preferentially near the front, whereas PTEN, Rho, ACA, and myosin-II are found near the rear of the cell (21–23). The G-protein coupled receptors are present mostly uniformly along the cell surface, though they apparently exhibit a slightly nonuniform distribution in strongly polarized cells (24,25). We focus on biochemical entities that are early in the polarization pathways, many of which are also involved in gradient sensing.

Much of the recent biochemical focus related to gradient sensing has been on phosphoinositide lipids (PI(3,4,5)P<sub>3</sub> and PI(3,4)P<sub>2</sub>) and the enzymes (PI3K and PTEN) that regulate them (26–28). Further regulation, related directly or indirectly to the actin cytoskeleton, contributes to a sharp localization of these lipids at the leading edge (12). The amplified production of these lipids relative to unstimulated cells arising from the dual contribution of PI3K and PTEN has been previously modeled (13,29). A model describing this dual regulation and relating it to adaptation to homogeneous stimulation has been previously presented (14).

To study the interaction of externally induced and intrinsic polarity, we employ qualitatively simplified, rather than detailed biochemical models, because many biochemical details that are most pertinent to this problem are not known (e.g., details regarding receptor regulation of PI3K, PTEN, regulation of  $G_\alpha$  and  $G_{\beta\gamma}$  proteins). The simplified models are motivated by known aspects of the biochemical pathways.

Our model includes signaling pathways corresponding to both receptor-mediated and intrinsic polarity: these regulate common biochemical components leading to motility. We first discuss various elements of the model and then present the underlying variables and equations.

## Receptor-mediated signaling

Our modeling framework incorporates two types of receptor-regulated pathways: global and local (Fig. 1 B). Local pathways are those where the extent of regulation of downstream components depends on the degree of local occupancy of receptors. In contrast, global pathways offer downstream regulation, dependent on receptor occupancy averaged over the cell periphery and involve components that are highly diffusible. Both local and global pathways can regulate downstream processes in either excitatory or inhibitory capacities. The combination of local and global pathways is able to account for gradient sensing and polarization consistent with adaptation to spatially homogeneous signals (30).

## Intrinsic polarity

How polarity arises independently of externally imposed gradients remains unclear. For example, in *Dictyostelium* cells, a change occurs during the developmental process (5).

Cells that are 4 h in the developmental process are, at best, weakly polarized: they do not have a clear and persistent separation of front and back. Though these cells are motile, they extend pseudopods in more-or-less random directions. In contrast, cells 7 h into development have sharp and persistent localization of various components at both ends of the cell.

The transition from unpolarized to a strongly polarized state may result from some kind of symmetry-breaking (31). It is possible to build models that give rise to a nonuniform steady state, representative of a persistent front and back, based on symmetry breaking (32–35). However, the symmetry breaking may not necessarily be induced by, or related to the chemotactic pathway. Moreover, there are different ways in which symmetry might break to give rise to polarity cues. It is possible that landmarks for polarity cues are established earlier in development (spatial symmetry breaking), and the polarity pathways are activated by another temporal signal later in development, as in *Saccharomyces cerevisiae* (20). To keep our approach as general as possible, we assume that the intrinsic polarity pathways are controlled by signals with concentration profiles that are localized at the front (*F*) and back (*B*). Below, we will consider how these signals may interact with receptor-mediated signaling.

## Model domain

Because most of the important reactions regulating chemotaxis take place on the cell membrane and cell cortex, we assume that all the elements of our model reside there. The spatial coordinate, *s*, corresponds to the arc-length of the membrane (see Fig. 1 *B*). We do not make use of cytosolic dynamics explicitly; these can also be incorporated in a simple manner by including an additional compartment that has transport to and from the membrane. Periodic boundary conditions are invoked. Though polarization involves a change of shape from an essentially circular cell to a more elongated cell (see Appendix A), we assume that this shape change is a downstream effect of the polarization of the various signaling components; possible feedback effects of shape change on the concentration profiles of the components will not be dealt with here. When we employ global entities, we assume that diffusion is through the cell membrane. This provides essentially the same kind of global regulation as the case where diffusion is cytosolic, and is sufficient for our purpose. In general, the time taken to recruit a species from the cytosol to the cell membrane through diffusion or any other transport limitations can be accounted for by a suitable choice of the corresponding rate constants.

## One-dimensional gradients

As chemotaxis and polarization occur in response to relatively simple concentration fields, such as those with variation in mainly one direction, we concentrate on this case in

detail. We assume a two-dimensional circular cell in the plane subject to a concentration field varying only in one direction. This one-dimensional variation allows us to address issues relating to the motility without having to consider the complexity associated with motility in higher dimensions. In this case, the cell either remains stationary or moves to either the left or right, depending on the net signal from the motility apparatus (described below). For cells whose shapes are surfaces of revolution, if the angular coordinate of an element of the surface is  $\theta$ , the symmetry of the cell shape and external concentration field implies that, for the receptor occupancy *R*,  $R(\theta) = R(-\theta)$  for  $-\pi \leq \theta \leq \pi$ . The symmetry condition implies that  $dR/d\theta = 0$  at  $\theta = 0, \pi$ ; equivalently,  $dR/ds = 0$  at the front and back of the cell.

## Turning mechanism

We need to incorporate into the model the ability of the cell to turn sharply in response to changing and/or unsuitable gradients (36–38). Because we do not model the mechanics of the cell in detail, we treat the turning of the cell in a phenomenological way. We incorporate a simple mechanism acting as a turning indicator. This is necessary to describe the response of a cell to an external gradient, even with variation in only one direction. The mechanism involves the interconversion of two components (*T* and *T\**) according to

$$\begin{aligned}\frac{dT}{dt} &= -k_t S \times T + k_{-t} T^*, \\ \frac{dT^*}{dt} &= k_t S \times T - k_{-t} T^*.\end{aligned}$$

The directional regulator signal, *S*, is related to the receptor signal by a local excitation, global inhibition mechanism (30); see Eq. 3 below. This mechanism determines a condition for the cell to turn that incorporates contributions from both the local concentration at the front, and the spatial average of the concentration around the cell. In our one-dimensional model, we make the cell reverse orientation instantaneously (i.e., *R(s)* is replaced by *R(l/2 – s)*) if the signal *T\** at the current “front” of the cell falls below a threshold value, *T<sub>cr</sub>*. The *T\** value is reset to its basal level whenever the cell turns. This mechanism allows for a cell to change direction abruptly, without necessarily rearranging its intrinsic polarity.

Thus, a cell moving in the direction opposite the direction of a strong enough gradient will eventually change its direction either by creating a new pseudopod at the current “back” of the cell (reorganization of polarity), or by turning abruptly based on this criterion. The rate constants *k<sub>t</sub>* and *k<sub>-t</sub>* quantify the sensitivity and tendency of the cell to turn: a cell may take either a relatively long (small *k<sub>t</sub>*, *k<sub>-t</sub>* relative to other rate constants) or short (large *k<sub>t</sub>* and *k<sub>-t</sub>*) time to decide to turn sharply. It is also possible to choose parameters so that the tendency of the cell to turn sharply in reasonable gradients is

suppressed (this is done by simply choosing a low enough value for  $T_{cr}$ ), in which case the only option for a cell to change direction is to reorganize its polarity. Thus, the incorporation of this module allows the model to exhibit a variety of responses to changing spatial and/or temporal signals, by variation of parameters.

### Model variables and equations

The model equations presented below describe signaling pathways from the receptor ( $R$ ) to a motility element ( $F_m$ ) via intermediate components (Fig. 1). The nature of signaling from the receptor involves both local ( $L$ ) and global ( $G$ ) pathways (14,30) regulating a signaling element ( $S$ ) that is able to account for adaptation to homogeneous stimuli:

$$\frac{\partial L}{\partial t} = k_l R(s) - k_{-l} L, \quad (1)$$

$$\frac{\partial G}{\partial t} = k_g R(s) - k_{-g} G + D_1 \frac{\partial^2 G}{\partial s^2}, \quad (2)$$

$$\frac{\partial S}{\partial t} = k_s L \times (1 - S) - k_{-s} G \times S. \quad (3)$$

These signals are responsible for regulation of further downstream frontness components  $F_1^*$ ,  $F_2^*$ , and  $F_m^*$ , representative of biochemical components PI3K, PI(3,4,5)P<sub>3</sub>/PI(3,4)P<sub>2</sub>, and F-actin, respectively; and backness component  $B_1^*$ , representative of PTEN.  $F_m^*$  is the motility signal that determines the direction of motion of the cell.

The equations

$$\frac{\partial F_1}{\partial t} = -k_p L \times F_1 + k_{-p} G \times F_1^* + D_2 \frac{\partial^2 F_1}{\partial s^2}, \quad (4)$$

$$\frac{\partial F_1^*}{\partial t} = +k_p L \times F_1 - k_{-p} G \times F_1^* + D_2 \frac{\partial^2 F_1^*}{\partial s^2}, \quad (5)$$

and

$$\frac{\partial B_1}{\partial t} = -k_q G \times B_1 + k_{-q} L \times B_1^* + D_3 \frac{\partial^2 B_1}{\partial s^2}, \quad (6)$$

$$\frac{\partial B_1^*}{\partial t} = +k_q G \times B_1 - k_{-q} L \times B_1^* + D_3 \frac{\partial^2 B_1^*}{\partial s^2}, \quad (7)$$

depict the receptor regulation of the frontness ( $F_1^*$ ) and backness ( $B_1^*$ ) components early in the polarization pathways (such as PI3K and PTEN), via a combination of local and global pathways, similar to those of Ma et al. (14). Though the local and global pathways regulating each of these components could be different, we will assume for simplicity that the respective local and global pathways have the same properties.

The signals  $F_1^*$  and  $B_1^*$  are propagated further down the pathways; the frontness pathways are governed by the equations

$$\frac{\partial F_2}{\partial t} = -k_r F_1^* F_2 + k_{-r} B_1^* F_2^* + D_4 \frac{\partial^2 F_2}{\partial s^2}, \quad (8)$$

$$\frac{\partial F_2^*}{\partial t} = +k_r F_1^* F_2 - k_{-r} B_1^* F_2^* + D_4 \frac{\partial^2 F_2^*}{\partial s^2}, \quad (9)$$

with similar equations for  $B_2$  and  $B_2^*$ . The regulation of the component  $F_2^*$  involves dual contributions from  $F_1$  and  $B_1$ , similar to the regulation of PI(3,4,5)P<sub>3</sub> and/or PI(3,4)P<sub>2</sub> by PI3K and PTEN. Finally, we assume the regulation of motility components  $F_m^*$  (representative of F-actin or related GTPases) by  $F_2^*$  in a feedforward manner:

$$\frac{\partial F_m}{\partial t} = -k_m F_2^* F_m + k_{-m} F_m^* + D_5 \frac{\partial^2 F_m}{\partial s^2}, \quad (10)$$

$$\frac{\partial F_m^*}{\partial t} = +k_m F_2^* F_m - k_{-m} F_m^* + D_5 \frac{\partial^2 F_m^*}{\partial s^2}. \quad (11)$$

The intrinsic polarity pathways are initiated by species that have localized concentration profiles at each end. The frontness cue, which is a species with a concentration profile  $F(s)$  localized near the front, controls a pathway that regulates the reaction involving the species  $F_1$  and  $F_1^*$ . The governing reactions of this intrinsic polarization pathway are given by the interconversion between components  $IF$  and  $IF^*$ . For simplicity, we assume these to be nondiffusible, leading to the equations

$$\frac{\partial IF}{\partial t} = -k_c F(s) IF + k_{-c} IF^*, \quad (12)$$

$$\frac{\partial IF^*}{\partial t} = +k_c F(s) IF - k_{-c} IF^*. \quad (13)$$

In the same way, the backness cue—a species with concentration profile  $B(s)$  localized to the rear—regulates backness pathways. The governing reactions of this pathway are given by

$$\frac{\partial IB}{\partial t} = -k_c B(s) IB + k_{-c} IB^*, \quad (14)$$

$$\frac{\partial IB^*}{\partial t} = +k_c B(s) IB - k_{-c} IB^*. \quad (15)$$

All equations are nondimensionalized using appropriate time (1 s), spatial (5  $\mu\text{m}$ ), and concentration (e.g., total  $F_1 + F_1^* = 1$  under basal conditions for variable  $F_1$ , etc.) scales. We employ an illustrative set of parameter values in our simulations (detailed parametric sensitivity analysis will be performed in a subsequent investigation). The diffusion coefficients for the species (except for the local and global pathways) correspond to values of 1–5  $\mu\text{m}^2/\text{s}$ . The higher diffusion coefficient for the global pathways results in these species quickly equilibrating at values corresponding to the spatial average of the receptor occupancy. Our simulations are performed by spatially discretizing the resulting partial differential equations, and integrating the resulting ordinary differential equations using the solver ode45 in MATLAB (The MathWorks, Natick, MA). Simulations are performed,

for any given level of intrinsic polarity, by allowing the network to reach a steady state with respect to that level of intrinsic polarity, and then introducing the gradient. The intrinsic variables are kept fixed, unless the receptor-mediated pathways inhibit them.

As our main focus in this study is on the relation between intrinsic and receptor-mediated polarization pathways, we use simplified models most relevant to this investigation. We omit a number of other features that may be relevant in actual cells, including static nonlinearities and thresholds in the pathways, oscillatory effects involved in cell motility signaling, a realistic description of the pseudopod, as well as shape change.

## RESULTS

We first consider the response of the receptor-mediated pathway under the assumption that the cell is not intrinsically polarized (Eqs. 1–11 above, corresponding to  $\alpha = \beta = 0$  in the equations below; see also Fig. 2). The steady-state response, which is a function only of the external concentration field, depends on the relative gradient as a consequence of signaling through a combination of local and global pathways (12,30,39). The frontness components are above their basal values in the front, and below them at the back; the opposite holds for the backness signals.

We also consider the effect of the intrinsic polarity pathway (Eqs. 12–15) when no external gradient is present (see Fig. 3). The intrinsic polarity components ( $IF^*$ ,  $IB^*$ ) become

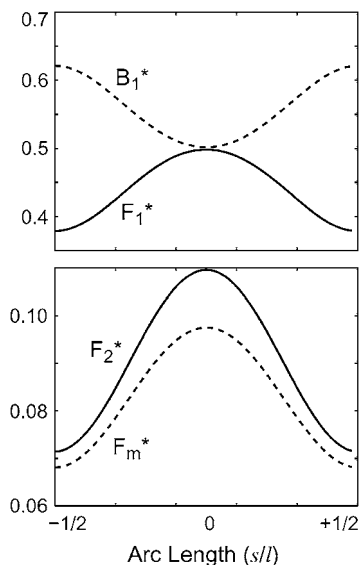


FIGURE 2 Polarity response in a gradient arising from receptor-mediated pathways. Shown is the network response along the perimeter of the cell to an external gradient  $R(s) = 0.8 + 0.2 \cos(2\pi s/l)$  assuming that the intrinsic pathways are inactive. The value  $s$  is the arc-length coordinate. Parameter values are  $k_1 = 0.8$ ,  $k_{-1} = 0.6$ ;  $k_g = 0.5$ ;  $k_{-g} = 0.3$ ;  $k_p = k_q = k_m = 1.0$ ;  $k_{-p} = k_{-q} = k_{-m} = 1.0$ ;  $k_s = 0.5$ ;  $k_{-s} = 4.0$ ;  $k_s = k_{-s} = 1.0$ ;  $k_i = 0.1$ ;  $k_{-i} = 0.1$ ;  $\gamma = 1.0$ ; and  $T_{cr} = 0.30$ . Diffusion coefficients are  $D_1 = 50$ ,  $D_2 = D_3 = D_4 = D_5 = 0.1$ .

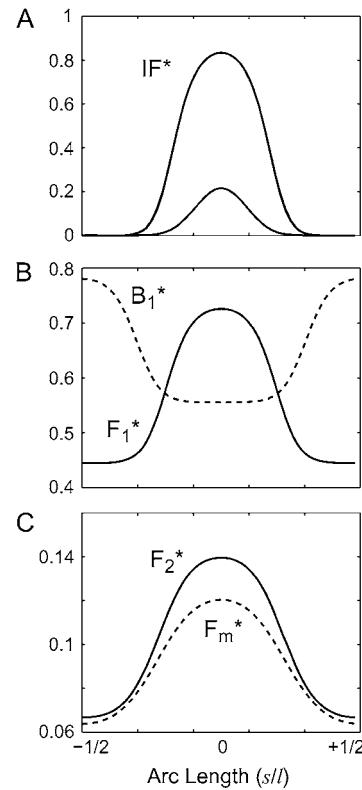


FIGURE 3 Polarity response arising from intrinsic pathways. (A) The intrinsic polarity component  $IF^*$  indicative of two different levels of intrinsic polarization. The higher curve corresponds to a maximum level of intrinsic polarization. (B,C) Downstream response in the network to the stronger of the two intrinsic polarity signals in panel A. Parameter values are  $k_c = k_{-c} = 0.0025$ ,  $k_{-c} = k_{-c} = 0.005$ ,  $\alpha = 3.0$ , and  $\beta = 3.0$ .

increasingly pronounced with the progression of intrinsic polarity (Fig. 3 A) and this affects all the downstream components (see Fig. 3, B and C).

We now examine different scenarios describing the interaction between the receptor-regulated and intrinsic pathways.

### Parallel regulation by receptor and intrinsic cues

We assume that receptor and intrinsic cues act in parallel (Fig. 4 A) and regulate common components in an additive manner. In this case, Eqs. 4–7 are replaced with

$$\begin{aligned} \frac{\partial F_1}{\partial t} &= -k_p L \times F_1 + k_{-p} G \times F_1^* - \alpha IF^* \times F_1 + D_2 \frac{\partial^2 F_1}{\partial s^2}, \\ \frac{\partial F_1^*}{\partial t} &= +k_p L \times F_1 - k_{-p} G \times F_1^* + \alpha IF^* \times F_1 + D_2 \frac{\partial^2 F_1^*}{\partial s^2}, \end{aligned}$$

and

$$\frac{\partial B_1}{\partial t} = -k_q G \times B_1 + k_{-q} L \times B_1^* - \beta IB^* \times B_1 + D_3 \frac{\partial^2 B_1}{\partial s^2},$$

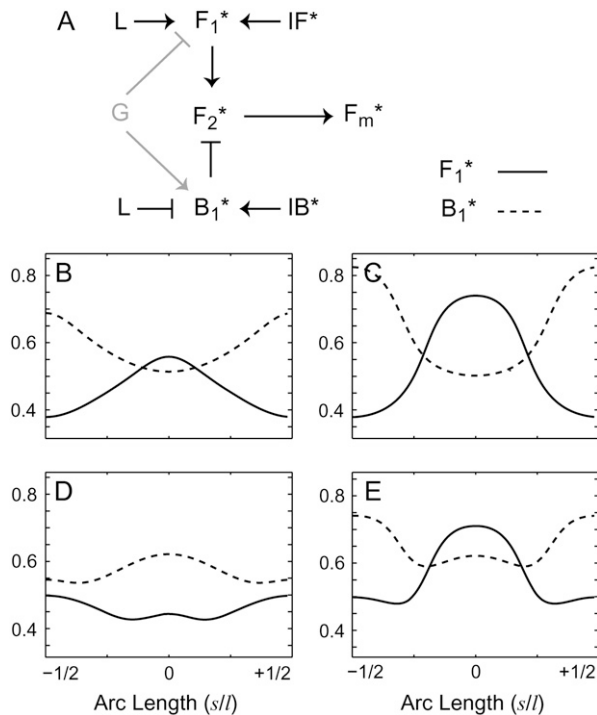


FIGURE 4 Polarity responses arising from a combination of intrinsic and receptor-mediated signals in anchored cells. (A) Schematic of the signaling pathway. The intrinsic polarization signals ( $IF$  and  $IB$ ) act in parallel of the receptor-mediated signals. (B–E) Front ( $F_1^*$ , solid) and rear ( $B_1^*$ , dashed) responses. (B) The quasi-steady response, when the cell is in the weaker of the intrinsic polarity states of Fig. 3 A, and an external gradient in the same direction is applied:  $R(s) = 0.8 + 0.2 \cos(2\pi s/l)$ . (C) The cell is in the stronger of the intrinsic polarity states of Fig. 3 A; the same gradient is applied. (D) With the weaker of the intrinsic polarity states, an external gradient in the opposite direction is applied:  $R(s) = 0.8 - 0.2 \cos(2\pi s/l)$ . The net response is correlated with the location of the receptor-mediated signal's maximum. (E) As in panel D, except the cell is in the stronger of the intrinsic polarity states. Note that the location of the net polarity response is opposite to that of the external signal. In all these cases, the concentration profiles of  $F_1^*$  and  $B_1^*$  lead to the polarization of downstream components  $F_2^*$  and  $F_m^*$ .

$$\frac{\partial B_1^*}{\partial t} = +k_q G \times B_1 - k_{-q} L \times B_1^* + \beta IB^* \times B_1 + D_3 \frac{\partial^2 B_1^*}{\partial s^2}.$$

The parameters  $\alpha$  and  $\beta$  describe the effect of intrinsic polarity on the frontness and backness components. The relative values of these parameters and those of the receptor-controlled pathways ( $k_p$ ,  $k_{-p}$ , etc.) determine the relative strengths of the two pathways in establishing a steady response; higher values denote a stronger contribution of the intrinsic polarity.

We first assume that cell is motionless. However, unlike cells that are immobilized through actin inhibitors (12,40), we assume that all signaling components are intact. We consider a scenario where this intact cell is anchored to the surface. This anchoring could be achieved by engineering the microenvironment of cultured cells causing them to

adhere to the surface (41). In our model, an anchored cell implies that it is subject to a static gradient and that it is incapable of turning (sharply); that is, the turning mechanism has no effect on the cell.

Whenever the external gradient is coaligned with the intrinsic polarity, the net result is that the external signal reinforces the intrinsic polarity and leads to stronger polarization than is possible from either (see Fig. 4, B and C). Note that for a fixed external gradient, the contribution of the receptor-controlled pathways need not necessarily be dominant. When an external gradient is imposed in a direction opposite to the intrinsic polarity, the two pathways work against each other (Fig. 4, D and E). The counteractive effects of the receptor controlled and intrinsic pathways are particularly acute when the external gradient cannot overcome the intrinsic polarity, which happens when the intrinsic polarity is strong (Fig. 4 E). In this case, the resulting steady-state profiles of  $F_1^*$  and  $B_1^*$  indicate a polarity opposite to the direction of the external gradient. An analytical description of parallel regulation by receptor-mediated and intrinsic cues is presented in Appendix A.

We now assume that the cell is not anchored to the surface, but is free to move and turn. This movement is assumed to be sufficiently slow so that the cell experiences an essentially static signal in the timescales of interest. Also, note that if the external gradient is in the same direction as the intrinsic polarity, the turning signal is not triggered and the effect is purely additive, so that the results are identical to those of the anchored cell (Fig. 4, B and C).

Different results arise, however, when the direction of the applied gradient is opposite to the cell's intrinsic polarity. If the intrinsic polarity is weak, then it is counteracted by the external gradient leading to net polarization in the direction of the applied gradient. Eventually, a stronger protrusive force develops in the rear— $F_m^*$  is greatest at  $s = \pm 1/2$  in Fig. 4 D—causing the cell to change its direction of motion by the gradual reorganization of polarity.

If the cell's intrinsic polarity is sufficiently strong, then the receptor-mediated pathways regulate the downstream pathways and attempt to reorganize its polarity. In this case, the turning mechanism induces the cell to turn sharply (flip); see Appendix A. This has the effect of aligning the intrinsic polarity with the external gradient. At this point, the net effect is reinforcement of the intrinsic polarity by the external gradient because, after turning, the profile is the same as when the external gradient's direction coincided with the intrinsic polarity (Fig. 4 C). This is true even though, initially, the external gradient was opposite to the intrinsic polarity.

For intermediate levels of intrinsic cell polarity, which effect—turning or protrusion at the old rear—dominates will depend on the relative timescales for meeting the turning threshold and for developing strong net protrusive force (correlated with concentration of  $F_m^*$ ) at the back of the cell. Clearly, an increase in the intrinsic polarity works in favor of turning, as opposed to the reorganization of polarity, because

the external signal has to counteract the existing inhibitory effect at the old rear of the cell. For a sufficiently polarized cell in a weak opposing gradient, turning sharply is its only option for chemotaxis. On the other hand, if the capability to turn is removed (as in an anchored cell), then the cell relies entirely on the reorganization of polarity by the gradient to change direction. In this case, a purely one-dimensional gradient of insufficient strength to counteract the intrinsic polarity will not be able to elicit a change in direction.

### Inhibition of intrinsic pathways by receptor pathways

In various contexts in polarity generation, it is assumed that external signals inhibit intrinsic cues (17,20). In our setting, we examine the possibility that receptor-mediated pathways inhibit intrinsic pathways while imposing their own contribution to downstream signaling components.

#### Direct local inhibition

The simplest possible receptor-mediated inhibition mechanism is a direct local inhibition of both intrinsic frontness and backness pathways (see Fig. 5 A). This inhibitory mechanism is incorporated into the dynamic equations of the components  $IF$ ,  $IF^*$ ,  $IB$ , and  $IB^*$  in a simple way, by replacing Eqs. 12–15 with

$$\begin{aligned}\frac{\partial IF}{\partial t} &= -k_c F(s)IF + k_{-c}IF^* + k_{if}R(s)IF^*, \\ \frac{\partial IF^*}{\partial t} &= +k_c F(s)IF - k_{-c}IF^* - k_{if}R(s)IF^*,\end{aligned}$$

and

$$\begin{aligned}\frac{\partial IB}{\partial t} &= -k_c B(s)IB + k_{-c}IB^* + k_{ib}R(s)IB^*, \\ \frac{\partial IB^*}{\partial t} &= +k_c B(s)IB - k_{-c}IB^* - k_{ib}R(s)IB^*.\end{aligned}$$

The extent of inhibition is determined by the rate constants  $k_{if}$ ,  $k_{ib}$ . In this direct scheme, increasing receptor occupancy uniformly through homogeneous stimulation inhibits the intrinsic frontness and backness pathways (Fig. 5 B). This inhibitory effect naturally leads to a decreased degree of polarity of downstream components such as  $F_1^*$ ,  $B_1^*$ ,  $F_2^*$ , and  $F_m^*$  (not shown). Moreover, an increase in the magnitude of the stimulus leads to greater reduction in cell polarity.

We note from the steady-state profiles

$$\begin{aligned}IF^*(s) &= k_c F(s)/(k_c F(s) + k_{-c} + k_{if}R(s)), \\ IB^*(s) &= k_c B(s)/(k_c B(s) + k_{-c} + k_{ib}R(s)),\end{aligned}$$

that local inhibition leads to the inhibition of intrinsic polarity components even in a gradient. In contrast to the purely additive case, coalignment of the external gradient with intrinsic polarity does not simply reinforce polarity. Instead, the result is a combination of the receptor-mediated

and inhibited intrinsic pathways, with inhibition effects being highest at the location where the external signal is maximum. Thus, disruption of the receptor-mediated pathways implies that a uniform stimulus still reduces intrinsic polarity. We also note that if  $k_{ib}$ ,  $k_{if} \gg k_c$ ,  $k_{-c}$ ,  $k_e$ , and  $k_{-e}$ , then the inhibition mechanism in a homogeneous external signal leads to the effective destruction of intrinsic polarity. Similar conclusions can be drawn for gradients too.

We note that if an inhibition mechanism is able to suppress the source of intrinsic cue formation itself, then homogeneous stimulation of sufficient magnitude could lead to the complete dismantling of the intrinsic polarity. In this case, receptor-mediated inhibition would lead to the network governing polarity cue formation being unable to sustain the stable formation/persistence of a cue (for example, the module in that parameter regime may not be capable of exhibiting inhomogeneous states). The net behavior would then be completely determined by the external signal, independent of the state of intrinsic polarity.

#### Inhibition involving local and global pathways

We now examine a more complex receptor-mediated inhibition mechanism involving both local and global pathways. We first note that if the inhibitory mechanism involves only global intermediates, the behavior in response to a uniform stimulus is essentially the same as that above under homogeneous stimulation and leads to a weakening of intrinsic polarity pathways and reduced polarity.

We consider an inhibitory mechanism that does not lead to any permanent inhibitory effect of intrinsic pathways when the cell is subject to homogeneous inputs (so that the inhibition disappears as the cell adapts to the homogeneous stimulus). The inhibitory signal is regulated by the receptor by a combination of local and global pathways (see Fig. 5 C). Representative equations are

$$\begin{aligned}\frac{\partial IF}{\partial t} &= -k_c F(s)IF + k_{-c}IF^* + k_{if}R_{Fin}(s)IF^*, \\ \frac{\partial IF^*}{\partial t} &= +k_c F(s)IF - k_{-c}IF^* - k_{if}R_{Fin}(s)IF^*,\end{aligned}$$

and

$$\begin{aligned}\frac{\partial IB}{\partial t} &= -k_c B(s)IB + k_{-c}IB^* + k_{ib}R_{Bin}(s)IB^*, \\ \frac{\partial IB^*}{\partial t} &= +k_c B(s)IB - k_{-c}IB^* - k_{ib}R_{Bin}(s)IB^*.\end{aligned}$$

The signals  $R_{Fin}$  and  $R_{Bin}$  describe the receptor-mediated inhibition of  $IF^*$  and  $IB^*$ . We can consider different scenarios in which such an inhibition could occur. In one such case, the inhibitory signal  $R_{Fin}$  results from the receptor via a local-inhibition, global-excitation mechanism, and the signal  $R_{Bin}$  results from a receptor pathway involving a local-excitation, global-inhibition mechanism. There are, of course, different combinations of local and global regulation of this

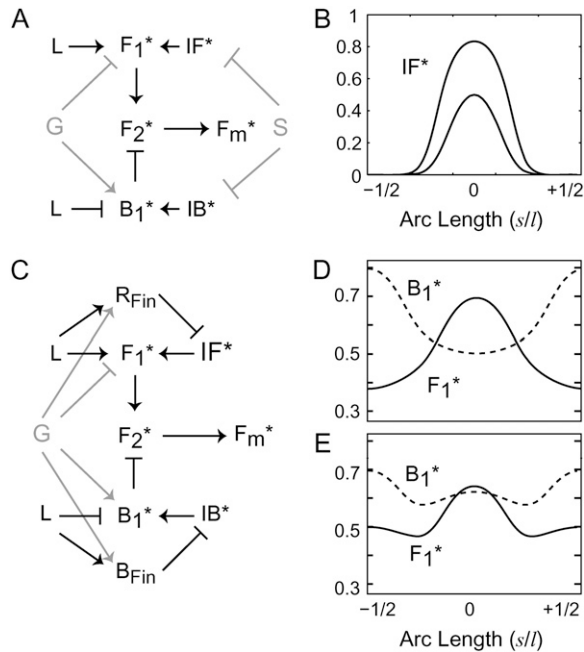


FIGURE 5 Receptor-mediated pathways inhibit intrinsic polarization pathways. The cell is originally possessed of a high level of intrinsic polarity ( $IF^*$  and  $IB^*$  corresponding to the *high* curve in Fig. 3 A). (A) Receptor-mediated pathways inhibit intrinsic polarization via local pathways. Thus, homogeneous stimulation results in a reduction of the intrinsic polarity signals  $IF^*$  (B) and  $IB^*$  (not shown), and this propagates to the downstream pathways. Parameter values are  $k_{if} = k_{ib} = 2.5$ ;  $k_c = k_{-c} = 2.5$ ;  $k_{-e} = k_e = 0.5$ , and the external homogeneous stimulation is  $R = 0.8$ . (C) Inhibition of intrinsic polarization by the receptor signals involves a combination of local and global pathways: here homogeneous stimulation would not result in a permanent effect on intrinsic polarization. Parameters are as in panel B; those of the local and global pathways are  $k_a = k_{-a} = k_b = k_{-b} = 1.0$ . In panel D, the external signal is  $R(s) = 0.8 + 0.2 \cos(2\pi s/l)$  and is in the same direction as the intrinsic polarity; in panel E, it is in the opposite direction:  $R(s) = 0.8 - 0.2 \cos(2\pi s/l)$ . The intrinsic polarity dominates in the latter case, but the net effect is not as strong as Fig. 4 E because of the inhibition of intrinsic pathways. Simulations were repeated for the case  $k_c = k_{-c} = 0.0025$ ,  $k_{-e} = k_e = 0.005$  (which corresponds to the same  $IF^*$  and  $IB^*$  profiles). In the case of local inhibition, the intrinsic polarity components  $IF^*$ ,  $IB^*$  are essentially nullified. Similarly in the case of complex inhibition depicted in panel C, the net result in any nonzero homogeneous stimulus is a very weak polarity; the behavior in a gradient also shows a small modulation of this weak polarity (see text).

inhibition mechanism, and they can all be analyzed in exactly the same way. The equations governing  $R_{Fin}$ ,  $R_{Bin}$  are

$$\begin{aligned}\frac{\partial R_{Bin}}{\partial t} &= -k_b L(1 - R_{Bin}) + k_{-b} G \times R_{Bin}, \\ \frac{\partial R_{Fin}}{\partial t} &= -k_a G(1 - R_{Fin}) + k_{-a} L \times R_{Fin}.\end{aligned}$$

In a gradient,  $R(s) = a + b \cos(2\pi s/l)$ , the steady-state profiles of these variables are

$$R_{Bin}(s) = \frac{k_b k_i k_{-g}(a + b \cos[2\pi s/l])}{k_b k_i k_{-g}(a + b \cos[2\pi s/l]) + k_{-b} k_g k_{-l} a},$$

$$R_{Fin}(s) = \frac{k_a k_g k_{-l} a}{k_a k_g k_{-l} a + k_{-a} k_i k_{-g}(a + b \cos[2\pi s/l])},$$

where we have used the fact that the global pathway is highly diffusible. From the steady-state expressions for  $IF^*$  and  $IB^*$ ,

$$IF^* = k_c F(s) / (k_c F(s) + k_{-c} + k_{if} R_{Fin}(s)),$$

$$IB^* = k_e B(s) / (k_e B(s) + k_{-e} + k_{ib} R_{Bin}(s)),$$

and noting the nature of regulation of  $R_{Fin}$ ,  $R_{Bin}$  by the receptor, we see that in homogeneous signals, this additional term contributes a constant value in the denominator independent of the external stimulus. In the case considered, in a gradient,  $R_{Fin}$  becomes less than its basal value (and attains its minimum) at the location where the external signal is maximum, and  $R_{Bin}$  becomes greater than its basal value (and attains its maximum) here. Thus, if the external gradient is coincident with the intrinsic polarity of an anchored cell, this inhibition actually reinforces the polarity; whereas when the external gradient is opposite to the direction of intrinsic polarity, this inhibitory mechanism does partially suppress intrinsic polarity (Fig. 5, D and E).

From the expressions for  $IB^*$  and  $IF^*$  above, we note that if  $k_{ib}$ ,  $k_{if} \gg k_c$ ,  $k_{-c}$ , and  $k_e$  and  $k_{-e}$ , then the equations for  $R_{Fin}$  and  $R_{Bin}$  enforce a state of weak intrinsic polarity. This is true under both the homogeneous stimulation ( $b = 0$ ), irrespective of strength (in which case  $R_{Fin}$  and  $R_{Bin}$  do not depend on  $a$ ), and in the gradients. Thus, for such a complex inhibition mechanism to work in gradients, we require that  $k_{ib}$  and  $k_{if}$  be of the same order as  $k_c$ ,  $k_{-c}$ ,  $k_e$ , and  $k_{-e}$ .

Because of the tendency to suppress the intrinsic polarity pathways, this inhibitory mechanism would tend to reduce, or delay the tendency of a polarized cell to turn sharply in this case, when compared to the case of no inhibition. Of course, it remains to be seen if such an inhibitory mechanism exists at all. Therefore, rather than vary the effect of such an inhibition, experiments that could point to the presence of such an inhibition would prove more useful. These effects could be detected by modifying receptor-controlled pathways of downstream components, such as PI3K. Thus, inhibiting the last component in the PI3K recruitment pathway starting from the receptor (which is not part of the intrinsic pathway), and subjecting a cell with some degree of intrinsic polarization to a gradient, would give useful information. If there was genuinely an inhibitory mechanism as described above, a gradient would affect the PI3K localization (which results from intrinsic pathways), even though the direct pathway leading from the receptor has been disrupted. Such experiments, however, require more biochemical knowledge regarding the receptor regulation of PI3K than is currently known.

In conclusion, it is certainly possible that inhibitory pathways emanating from the receptor could impact upon intrinsic pathways. However, the presence or absence of such pathways may not be easily directly discerned. Inhibitory pathways that are either local or global (but not both)



could be detected by experiments that focus on the effect of a homogeneous stimulus on intrinsic polarity components. However, if the inhibition were to involve local and global pathways, and itself adapt to homogeneous inputs, the only way of proving its presence would be to perform experiments in gradients, by comparing regular cells and cells where the direct receptor controlled pathway was disrupted.

## CONCLUSIONS AND DISCUSSION

Much of the recent attention in eukaryotic chemotaxis at the single-cell level has been on the process of gradient sensing. To connect gradient sensing to chemotaxis and migration in these cells, a number of important issues need to be addressed. Among these is a thorough understanding of the relation and interaction between gradient sensing and cell polarization, and the role of the actin cytoskeleton therein.

We have focused on some core issues related to polarity, the process by which different signaling components localize at opposite ends of the cell persistently, along with any attendant morphological change (5,16,26,42–44). This definition includes the ability of the cell to polarize in the absence of externally imposed gradients. We described a modeling framework to analyze how this inherent polarity can be reconciled with that induced by externally imposed chemoattractant gradients.

One example of an intrinsic polarization process is that which occurs during *Dictyostelium* development: cells 7 h into the developmental cycle are strongly polarized (36,45). Our modeling framework deals with different ways in which such an intrinsic polarization process may be exploited by the chemotactic pathways. Thus, we formulated our framework to deal with the relationship between the intrinsic and chemotactically induced polarity processes, and addressed different questions regarding their interaction. While our modeling framework was constructed in a specific setting, its insights are relevant to other systems/situations involving competing polarity mechanisms.

Our modeling framework includes only the most important aspects of signaling pathways and information flow in the actual system, relevant to the issues at hand. This allowed us to deal with the main questions of interest and relate some core hypotheses to implications in a transparent manner. Our framework was qualitatively simplified rather than detailed biochemical since many relevant biochemical details, such as the dynamics and regulation of the  $G_\alpha$  and the  $G_{\beta\gamma}$  proteins, as well as the regulation of Raps, PI3K, and PTEN by the receptor, are still under experimental investigation. We also did not incorporate change in morphology, feedforward nonlinearities and thresholds in signaling, a realistic description of a pseudopod, or oscillatory effects in motility signaling. These aspects will be dealt with in future studies.

The model was formulated on a membrane of a two-dimensional representation of a cell exposed to a one-dimensional external gradient that is able to induce chemotaxis

and polarization. This restriction allows us to treat motility in a simple manner. Different aspects of motility in the one-dimensional setting have been previously studied (46,47). We also incorporated, in a phenomenological manner, a mechanism describing the cells' ability to turn sharply when faced with a changing and/or unsuitable gradient—a behavior that has been observed in both strongly polarized neutrophils and *Dictyostelium* cells (36). This was accomplished by the incorporation of a “turning module.” Different parameters in this module allow for the possibility of sharp turning, and also for its abolition. We modeled the initiation and progression of intrinsic polarity, as controlled by some polarity cues that were described phenomenologically.

We considered different scenarios regarding the interaction of intrinsic and externally induced polarity pathways. In the first case, we assumed that these pathways act in parallel and regulate common downstream components (Fig. 4). The implications of this possibility were most transparent when the intrinsic pathway dynamics are much slower than those of the receptor-controlled pathways. Stimulation of a cell, anchored to the surface but otherwise intact, led to additive effects: if the gradient was in the same direction as the intrinsic polarity, stronger polarity ensues. In contrast, a gradient in the opposite direction acted to counteract the intrinsic polarity. Thus, cells that have sufficiently strong intrinsic polarization do not reorganize their polarity in response to weak external gradients, so that the net resulting polarity was opposite to that of the external gradient. In contrast, motile cells with sufficiently strong intrinsic polarization changed direction when exposed to a gradient in the opposite direction as a result of the competition between the tendencies of the cell to reorganize its polarity and then to turn sharply. For strongly (intrinsic) polarized cells, turning dominates because of the greater time taken to reorganize polarity.

The parallel action of externally induced and intrinsic pathways has important implications for chemotaxis. It suggests that cells with sufficiently strong intrinsic polarity can respond to relatively weak gradients only by reorienting themselves appropriately and not by the reorganization of their polarity. This is also relevant to the cell's response to multiple sources/chemotactic cues: the history of the cell's exposure to these cues and the location of these cues relative to the front of the cell is crucial in determining the cell's response. Thus, the nature of the response is different from that in immobilized cells (39) and weakly polarized cells.

We also considered an implicit assumption made in different contexts that extrinsic polarity effects (receptor-mediated pathways in this context) suppress intrinsic ones (Fig. 5). The simplest scenario examined was one involving direct local inhibition of intrinsic pathways. This assumption implies that homogeneous stimulation of intrinsically polarized cells leads to a reduction in the concentration of intrinsic polarity components and, hence, overall polarity, and that the extent of reduction of polarity depended on the degree of stimulation. We also considered the possibility that the

suppression could occur downstream of an adaptation mechanism, in which case, spatially homogeneous stimulation would have minimal effect in suppressing intrinsic pathways. In this case, depending on the manner of the suppression, the net polarity in a gradient emerges from the combination of external and intrinsic pathways in a nontrivial way. Experiments performed with gradients imposed in the same and opposite direction as the intrinsic polarity could test the presence/absence of such suppressive pathways.

While feedforward nonlinearities, feedback, and other interactions affect signal propagation in the polarity pathways, the inclusion of these effects does not alter our main conclusions. This is because the critical issue remains as to how the intrinsic and receptor-mediated signals are coupled.

Finally, it is worth considering the possible role of nonlinear dynamic transitions in polarization and chemotaxis (see Appendix B). Other models of eukaryotic gradient sensing employ nonlinear dynamic transitions to describe the origin of polarization in homogeneous stimulation, and the same nonlinear dynamic transition is at the core of the amplification effects in gradient sensing (9,10,32). In *Dictyostelium*, the basal state is always one in which the cell is moving, even if the cells are weakly polarized. Weakly polarized cells move by extending pseudopods in apparently random directions. The homogeneous stimulation of these cells does not lead to strong persistent polarization but instead results in a degree of polarization that is essentially the same as before stimulation. Thus, unlike the scenario described by the aforementioned models, we do not have a situation where homogeneous stimulation necessarily orchestrates a nonlinear dynamic transition leading to a strongly polarized state. We note that it is possible that homogeneous stimulation could actually regulate the signaling system so that it transiently passes through a parameter regime that supports multiple asymptotic states, but we know of no corroborating experimental evidence yet.

We investigated whether nonlinear dynamic transitions could occur in the propagation of polarization. As demonstrated in Appendix B, a spatially varying receptor signal is able to induce multiple steady states as a result of the interplay between nonlinearities and heterogeneity, and activate a transition. With upstream regulation of this mechanism arising from a combination of local and global pathways, it is possible for such a nonlinear transition to be involved in signal propagation either at the front or at the back of the cell. While some pattern-forming process may be responsible for the creation of intrinsic polarization, we see from this article that it is entirely possible that this process is not directly exploited by the chemotactic pathways.

Our results demonstrate the need for systematic experimental investigations contrasting the relative effects of intrinsic and external pathways on both frontness and backness components. This entails performing experiments with the same imposed gradients on cells at different stages of their developmental state, for example. Systematically varying the

external gradient and measuring the response of the cells is also important. It is also important to work with static external gradients. Gradients established in microfluidic devices may be especially useful here (48,49). The clearest way to address various related issues is to perform experiments on cells that are anchored, thus preventing or minimizing motility without impairing the actin cytoskeleton. Environments where the cells are made to adhere strongly to the surface and/or changing surface properties to minimize movement could prove particularly useful (41). Investigating the response of such cells to homogeneous increases and decreases in receptor stimulation provides further important information. These experimental settings would allow for a clearer investigation of the roles of intrinsic and receptor-mediated pathways than experiments performed with transient external signals and moving cells. Such controlled experiments would provide invaluable information on how the response of migrating cells depends on both signal detection and their intrinsic state. Experimentally checking for the presence of a nonlinear dynamic transition is more difficult, especially if homogeneous stimulation does not yield useful information. The signature of a nonlinear transition would be a discontinuous response as the gradient is varied.

For the most part, we have sidestepped the issue of what processes may be involved in generating the intrinsic polarity cues. This would involve symmetry breaking, but the crucial issue is related to the exact stage where the symmetry breaks, and whether this is at all related to chemotaxis. Employing a concrete model for symmetry breaking, similar to that of Narang (32) to describe the generation of intrinsic cues, does not alter our main conclusions.

Polarity generation is a complex and subtle process. In this article, we have constructed a simplified model as a first step to address this complex problem. Nevertheless, several issues remain to be addressed. For example, how the intrinsic polarity cues generated, and whether they depend on an intact actin cytoskeleton. Thus, the role of adding actin inhibitors to cells at different stages of development (and in general, in different stages of intrinsic polarity) needs to be studied systematically. In our model, we have assumed that we are working with cells with an intact cytoskeleton in which the developmental process or any other progression of intrinsic polarity is unimpaired.

An additional aspect that deserves special attention is the origin of an apparent random motility in essentially unpolarized cells. It appears that there is an intrinsic process that is responsible for this seemingly random pseudopod generation, and this is functional even in cells where the receptor is not expressed (50). However, this process is overridden by gradients in weakly polarized cells. Recent experiments have suggested that small levels of chemoattractant induce random pseudopod extension leading to random cell motility (51). However, this cannot explain how cells lacking the receptor extend pseudopods randomly (50). We further note that even if a low level of chemoattractant were to cause

symmetry breaking, resulting in the transition from a completely immobile cell to a mobile cell with pseudopod extension, it does not result in a strong and persistent polarity as produced, for example, during development. In our work, we assume that there is always a small basal amount of chemoattractant.

A systematic experimental and theoretical investigation of the interaction between chemotactic signals and intrinsic polarity is of critical importance in understanding chemotaxis. The extent to which this differs between eukaryotes would shed light on how and to what extent cells might employ this intrinsic capacity for chemotaxis. Finally, this also provides an example of interaction of different cues in polarization, which could have analogs in developing and other biological systems.

## APPENDIX A: ANALYSIS OF PARALLEL REGULATION BY RECEPTOR-MEDIATED AND INTRINSIC CUES

Insight into the parallel regulation of downstream pathways by receptor-mediated and intrinsic cues can be obtained by examining analytical expressions for the profiles of various downstream elements. We consider the case of parallel regulation, in the limiting case where the diffusion coefficients are  $D_2 = D_3 = D_4 = D_5 = 0$ . In this case, analytical expressions for steady-state profiles of the components of the polarity pathways  $F_1^*$ ,  $B_1^*$ ,  $F_2^*$ ,  $F_m^*$  can be obtained.

We assume that the dynamics of the intrinsic polarity is slow on the timescales of interest, so that the profile  $IF^*$ ,  $IB^*$  can be treated as quasi-steady. Based on the nondimensionalization of variables, and the fact that the upstream pathways affect only the interconversion of  $F_1$ ,  $F_1^*$  and  $B_1$ ,  $B_1^*$ , it is easy to see that  $F_1 + F_1^* = 1$ ,  $B_1 + B_1^* = 1$ . The steady-state equilibrium conditions for  $F_1^*$ ,  $B_1^*$  are

$$\begin{aligned} F_1^*/F_1 &= (k_p L + \alpha IF^*)/(k_{-p} G), \\ B_1^*/B_1 &= (k_q G + \beta IB^*)/(k_{-q} L). \end{aligned}$$

The steady-state profiles of the pathways  $L$ ,  $G$  in a (nonzero) external signal assuming highly diffusible global pathways are  $L = k_{ll}R$  and  $G = k_{gg}\langle R \rangle$ , where  $k_{gg} = k_g/k_{-g}$  and  $k_{ll} = k_l/k_{-l}$  and  $\langle \cdot \rangle$  denotes spatial average over the circumference of the cell. Thus, the steady-state profiles of  $F_1^*$ ,  $B_1^*$  are

$$\begin{aligned} F_1^* &= (k_p k_{ll} R + \alpha IF^*)/(k_p k_{ll} R + \alpha IF^* + k_{-p} k_{gg} \langle R \rangle), \\ B_1^* &= (k_q k_{gg} \langle R \rangle + \beta IB^*)/(k_q k_{gg} \langle R \rangle + \beta IB^* + k_{-q} k_{ll} R). \end{aligned}$$

The profiles of downstream components are then easily obtained as

$$\begin{aligned} F_2^* &= k_s F_1^*/(k_s F_1^* + k_{-s} B_1^*) \\ F_m^* &= k_m F_2^*/(k_m F_2^* + k_{-m}) \end{aligned}$$

from the profiles of  $F_1^*$ ,  $B_1^*$  above. The expressions for the profiles  $F_1^*$ ,  $B_1^*$  in particular give insight into the coupling between the pathways. We note that  $IF^*(IB^*)$  is a profile which is localized near the front(back), and has zero or close-to-zero concentration far away from the front(back).

Further insight can be obtained by substituting expressions for the external gradient, and the intrinsic polarity signals. A linear external signal can be described by the expression  $R(s) = a + b \cos(2\pi s/l)$ . For illustrative purposes and analytical insight, we use representative expressions for localized intrinsic polarity variables as  $IF^* = a_f \exp(-s^2/d^2)$  and  $IB^* = a_b$

$\exp(-(s - l/2)^2/d^2)$ . In these expressions, the condition that  $d \ll l/2$  is implicit, so that the each relevant intrinsic polarity variable is localized near each end, and hence these signals are effectively of zero strength far away from the relevant ends. Replacing these expressions into the relevant equations results in

$$\begin{aligned} F_1^*(s) &= \frac{k_p k_{ll} (a + b \cos[2\pi s/l]) + \alpha a_f \exp(-s^2/d^2)}{k_p k_{ll} (a + b \cos[2\pi s/l]) + \alpha a_f \exp(-s^2/d^2) + k_{-p} k_{gg} a}, \\ B_1^*(s) &= \frac{k_q k_{gg} a + \beta a_b \exp(-(s - l/2)^2/d^2)}{k_q k_{gg} a + \beta a_b \exp(-(s - l/2)^2/d^2) + k_{-q} k_{ll} (a + b \cos[2\pi s/l])}. \end{aligned}$$

These expressions determine the effective response of  $F_1^*$ ,  $B_1^*$ . We can consider the cases where  $b > 0$  (coincident intrinsic and receptor-mediated polarity) and  $b < 0$  (opposing intrinsic and receptor-mediated polarity).

First, if  $\alpha = \beta = 0$ , so that the cell has no intrinsic polarity, then  $F_1^*$ ,  $B_1^*$  both exhibit perfect adaptation to homogeneous signals, with an equilibrium value independent of the level of stimulus. This is seen in the above expressions, where  $b = 0$ : the dependence on  $a$  drops out. Small values of the coupling parameters  $\alpha$ ,  $\beta$  result in small perturbations of this scenario. This is also the case for weak levels of the intrinsic polarity (i.e., small values of  $a_f$  and  $a_b$ ). For other values of the coupling parameters, the steady-state profiles depend on both the level of the external signal ( $R$ ) and the level of intrinsic polarity ( $IF^*$ ,  $IB^*$ ). We note, however, that when the profiles of  $IF^*$  and  $IB^*$  are sharply localized spatially, then outside these regions, the steady state will be essentially independent of the level of external stimulus.

Higher values of the coupling parameter lead to less relative dependence on the value of the external homogeneous signal, for a fixed level of intrinsic polarity. Here again, since the profiles of  $IF^*$  and  $IB^*$  are localized, there are regions far away from the front and back that equilibrate at levels essentially independent of the external signal.

These expressions also reveal the effect of external gradients. The steady state of  $F_1^*$  shows the additive influence of the intrinsic polarity, which is stronger either as the coupling parameter or the level of intrinsic polarity variable  $a_f$  increases; exactly the same conclusion can be made for  $IB^*$ . Again, the expressions also make transparent how a weak gradient is unable to effectively oppose a strong intrinsic polarity and in general, how the strength of the gradient as well as the strength of the intrinsic polarity variables combine to determine an effective response.

## Effects of intrinsic polarization on adaptation

We have examined the interaction of the receptor-mediated and intrinsic pathways under both homogeneous and spatially varying stimuli. A central point has been the fact that certain receptor-mediated pathways lead to an adaptive response. In our modeling framework, we examined in detail how parallel additive regulation of receptor-mediated and intrinsic pathways could affect downstream pathways.

The additive regulation occurs via the variables  $F_1^*$  and  $B_1^*$ . The way in which the additive mechanism was constructed results in the property of perfect adaptation being lost as intrinsic polarity becomes stronger. We now demonstrate that, depending on the nature of the integration of the adaptive and intrinsic mechanism, the exact adaptation property can be retained.

Consider a frontness variable regulated by the receptor in exactly the same way as the variable  $F_1^*$ :

$$\begin{aligned} \frac{\partial F_0}{\partial t} &= -k_p L \times F_0 + k_{-p} G \times F_0^* + D_0 \frac{\partial^2 F_0}{\partial s^2}, \\ \frac{\partial F_0^*}{\partial t} &= +k_p L \times F_0 - k_{-p} G \times F_0^* + D_0 \frac{\partial^2 F_0^*}{\partial s^2}. \end{aligned}$$

By construction,  $F_0$  is a frontness signal that is also able to adapt to homogeneous signals. We now incorporate the additive regulation with intrinsic polarity at the next step:

$$\begin{aligned}\frac{\partial F_1}{\partial t} &= -k_{f1}F_0^* \times F_1 - \alpha IF^* \times F_1 + k_{m1}F_1^* + D_2 \frac{\partial^2 F_0}{\partial s^2}, \\ \frac{\partial F_1^*}{\partial t} &= +k_{f1}F_0^* \times F_1 + \alpha IF^* \times F_1 - k_{m1}F_1^* + D_2 \frac{\partial^2 F_1^*}{\partial s^2}.\end{aligned}$$

When the cell is subject to homogeneous stimulation, the steady state is obtained from the above equation, where the steady value of  $F_0^*$  is substituted. Because this does not depend on the value of the external signal  $R$ , neither does the resulting profile of  $F_1^*$ . An exactly analogous argument can be made for  $B_1^*$ . Thus, depending on how the adaptation and intrinsic polarity processes are integrated, it is possible to preserve the exact adaptation property for downstream variables subject to both these influences. In this scenario, adaptation occurs before the integration of receptor-mediated and intrinsic polarity. Thus, in this case and irrespective of the degree of intrinsic polarity, the cell can show perfect adaptation to homogeneous signals.

## Turning signal

We now demonstrate that, as discussed in the main text, the turning mechanism can be triggered in a cell with sufficiently strong intrinsic polarization that experiences a gradient in the opposite direction. This is seen by examining the steady state of the turning indicator:  $T^* = S/(k_{-I}/k_I + S)$ , where the steady-state value of  $S$  is  $S = k_s k_{II}(a + b)/(k_s k_{II}(a + b) + k_{-s} k_{gg} a)$ . In the absence of a gradient ( $b = 0$ ), the corresponding  $T^*$  is above the threshold  $T_{cr}$ . If the cell is polarized in a direction opposite to the external gradient ( $b < 0$ ), then the corresponding  $S$  and  $T$  are below their basal level. In sufficiently large gradients—as in the case of the simulation of Fig. 4—the latter can be made to fall below  $T_{cr}$ . Thus, unless the polarity of the cell is itself reorganized during the course of attaining its steady state, the variable in the turning module  $T^*$  will trigger the decision to reverse direction.

## Effect of cell shape and size

The above expressions can also be used to analyze the dependence of response of the networks on cell size and shape. In general, the dependence of cell size and shape occurs through the receptor occupancy signal, for a fixed external field. For a change in cell shape, the receptor occupancy changes from a cosine signal. We considered the effect of a change of shape from a circle (sphere) to a geometry corresponding to a rectangular (cylindrical) center (of length  $d$ ) with circular (spherical) caps of radius  $r_0$  at the front and back. This was compared to a circular cell with the same front to back distance in the same concentration field (i.e., same gradient and midplane concentration). Calculations analogous to those above show that the essential features and behavior are unaffected by this shape change. In fact, the peak values of the frontness and backness variables at the front and back are unaffected. The profiles are slightly altered owing to a change in curvature, but all the main conclusions of our study hold.

## APPENDIX B: NONLINEAR DYNAMIC EFFECTS IN THE POLARIZATION PATHWAYS

Here we examine some critical issues in gradient sensing and polarity generation: the possible role of nonlinear dynamic effects. This is relevant in this context for more than one reason. First, symmetry-breaking and pattern formation may play an important role in determining intrinsic polarity. Second, the role of nonlinear dynamic transitions lying at the heart of the chemotactic sensing process has been suggested (9,32). In fact, it was some of these questions that led us to formulate our modeling framework as one

dealing with the interaction of receptor-mediated and intrinsic polarity. It is natural to ask a number of nonlinear dynamic-centric questions in this context: what kind of nonlinear dynamic processes could be responsible for intrinsic cue generation? Are these exploited by the receptor-controlled pathways? Can nonlinear dynamic transitions be involved in the propagation of polarization pathways? Is it possible for a nonlinear dynamic transition to be consistent with adaptation to homogeneous stimulation?

We start by examining whether it is possible for nonlinear dynamic transitions to be involved in the propagation of polarization. A characteristic feature of many nonlinear systems is that they exhibit multiple attractors; that is, the system can reach different states asymptotically by varying only the initial conditions. Thus, we focus on the system changing attractors, but we do not consider essentially static nonlinear effects that may have an important effect in amplification or relative input-output response (see (8,13,14)). We then address the question whether it is possible that the polarization pathways can involve a nonlinear transition, even if there is no evidence of one when the cell is subject to homogeneous stimulation. We show that the answer is yes.

We demonstrate the possibility of the existence of nonlinear dynamic transition in polarization pathways by means of a simplified mechanism involving a single diffusible component described by

$$\frac{\partial v}{\partial t} = kv(1-v)(v-a) - \alpha(s)v + D \frac{\partial^2 v}{\partial s^2}.$$

This is posed on a one-dimensional region (i.e., membrane) and periodic boundary conditions are imposed. The receptor signal is incorporated into  $\alpha(s)$ . For purposes of illustration, we assume that  $\alpha(s) = c - b \cos(\pi s/l)$ . Under basal conditions,  $\alpha(s)$  is assumed spatially homogeneous ( $b = 0$ ). We choose the parameters  $c = 0.235$ ,  $k = 1$ ,  $D = 0.01$ , and  $a = 0.2$ .

We first note that the homogeneous steady states are given by  $v = 0$ , as well as solutions to the equation  $k(1-v)(v-a) = \alpha$ , which has real roots only when  $(a-1)^2 \geq 4\alpha/k$ . For the parameters chosen, this translates to  $\alpha \leq 0.16$ . Thus,  $\alpha = 0.16$  corresponds to the transition between monostability and bistability.

We now assume that  $\alpha$  varies spatially, and this is parameterized by the parameter  $b$ . In this system, information from the receptor is encoded in the dynamics of the parameter  $\alpha$  (discussed below). We first perform simulations starting from  $v = 1$ . When  $b = 0.08$ , there are regions (i.e., values of  $s$ ) where the kinetics exhibit the property of bistability; these correspond to a local value of  $\alpha$  decreasing below the critical value of 0.16. By performing the simulation where  $v$  is nondiffusible ( $D = 0$ ), we see that the net steady state attained shows the effect of this bistability: there is a region where the steady-state concentration of  $v$  is high, and everywhere else this concentration is 0 (Fig. 6 A).

However, repeating the simulation with diffusion present leads to a zero steady state everywhere (Fig. 6 A). This is a consequence of the so-called Maxwell condition (52) in spatially uniform bistable media: if an initial condition is chosen so that a small region is at one stable steady state, and the surrounding region is at another (stable) steady state, then generically one of these steady states “wins”. Either the small region expands to cover the entire medium, or it is “swallowed up” by the surrounding medium (as is seen here). The Maxwell condition for a spatially uniform bistable medium described by  $u_t = f(u) + u_{xx}$ , with homogeneous steady states  $u = u_0, u_1$  is given by  $\int_{u_0}^{u_1} f(u) du = \gamma \int (u_x^2/2) dx$ . The quantity  $\gamma$  is a scaled version of the speed of the front connecting the two steady states and its sign determines which of the homogeneous steady states emerges as dominant.

Although our mechanism is a spatially heterogeneous version of a bistable medium, and is in fact not even bistable everywhere, essentially the same effect is found here. The localized region of the higher steady state is consumed by the lower steady state. Increasing the heterogeneity amplitude further ( $b = 0.12$ ) leads to a steady state with a region of high  $v$ , even though  $v$  diffuses (Fig. 6 B). In this region, which is narrower than that where bistability exists, the Maxwell area condition is favorable for the upper steady state. Note that because the system is spatially varying, the attainment

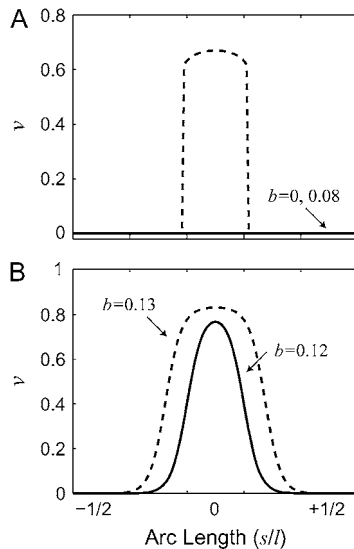


FIGURE 6 Spatial gradient can trigger a nonlinear dynamic transition. Steady state of the nonlinear mechanism described in Appendix B, starting from initial condition  $v = 1$ . Parameters are  $k = 1$ ,  $a = 0.2$ ,  $D = 0.01$ , and  $\alpha(s) = 0.235 - b \cos(2\pi s/l)$ . (A) When  $b = 0$ , the resulting steady state is the solution  $v = 0$  (solid line). Though a local bistability is present in the kinetics in certain parts of the domain when  $b = 0.08$ , the steady-state solution is still  $v = 0$ . However, a heterogeneous profile is seen for this value of  $b$  when  $D = 0$  (dashed). (B) Increasing  $b$  to 0.12 (solid) or 0.13 (dashed) leads to a heterogeneous profile for  $v$  resulting from a combination of the heterogeneous profile of  $\alpha$  and a nonlinear transition.

of an amplified steady state does not precisely correlate with a favorable Maxwell condition; there has to be a big enough spatial region where this condition is favorable. Increasing the heterogeneity amplitude even further ( $b = 0.13$ ) shows a broader spatial region where the effect of the nonlinear transition is felt. Thus, we have shown a genuine nonlinear transition with just a single component.

Building on this mechanism, we address two remaining issues. The first is the creation of a suitable initial burst in  $v$  so that the system can effectively employ any bistability that results. This is easily accomplished by adding an extra term in the equation

$$\frac{\partial v}{\partial t} = kv(1-v)(v-a) - \alpha(s)v + g(x,t) + D\frac{\partial^2 v}{\partial s^2}.$$

Initially,  $g(x, t) = 0$ , but undergoes a transient burst after stimulation before returning to its prestimulus level. This burst is sufficient to induce a transient jump in  $v$ , so that it can effectively “jump attractors.” Note that  $v = 1$  is not a steady basal state; the inclusion of this additional term allows the system to reach the same steady state as above starting from the homogeneous steady state  $v = 0$ . This effect could alternatively also be accomplished by suitably adjusting the temporal regulation of  $\alpha$  by the receptor.

The remaining issue is how this mechanism might be regulated by the receptor. The parameter  $\alpha(s)$  may be regulated by the receptor using a combination of local and global pathways. In contrast, the bursting term can be controlled by purely local or global pathways. In this case, homogeneous stimulation would allow  $\alpha$  to regain its original value at steady state. In a gradient,  $\alpha$  shows a graded profile. The homogeneous stimulation of the cell would lead to adaptation (as long as basal conditions are chosen so that the kinetics is in a monostable regime, this is guaranteed). An inhomogeneous stimulation of the cell (of sufficient inhomogeneity amplitude) would lead to a genuine nonlinear dynamic transition. We note that the heterogeneity induced in this mechanism is not an inherent one, but arises from upstream signals.

We can make a number of conclusions from this mechanism. First, the regulation of the parameter  $\alpha$  by the receptor using a combination of local and global pathways leads to adaptation in homogeneous stimulation with no permanent difference, while a gradient can cause a genuine nonlinear dynamic transition. Thus, it is possible for nonlinear dynamic transitions to occur in polarization pathways consistent with adaptation to homogeneous signals. The above analysis also shows that it is possible for a nonlinear transition to be involved in either the frontness or backness pathways. Second, depending on what combination of local and global pathways are involved in regulating the parameter  $\alpha$ , a transient increase or decrease in this parameter in homogeneous stimulation can be correlated with a nonlinear transition at the leading edge in a gradient. For example, regulation of  $\alpha$  by a combination of local, fast excitation and global, slow inhibition leads to a transient increase in homogeneous stimulation and a nonlinear transition at the leading edge. Equivalently, a transient increase in the parameter  $\alpha$  in a uniform stimulus could be associated with a nonlinear transition either at the front or back of the cell. Third, a removal of the external gradient causes the system to revert to the original state. Finally, a one-species system that is bistable and heterogeneous can indeed sustain multiple steady states in different regions, even though the species is diffusible. This property is not (generically) shared by one component spatially homogeneous bistable systems. Thus, it is possible to orchestrate a bistable transition without requiring additional diffusible inhibitors.

This discussion demonstrates that it is possible for nonlinear dynamic effects to play important roles in polarization pathways, with no signature of them being observed in homogeneous stimulation.

## Nonlinear dynamic and pattern-forming mechanisms in gradient detection

The latter models of Narang and co-workers (9,10,32) invoke strong nonlinear dynamic effects at the core of the gradient sensing pathways and are aimed at capturing a phenomenon observed in some systems: the fact that a homogeneous stimulation of the cells can lead to a persistent response and polarization in some (apparently random) direction. This behavior is observed in neutrophils that are treated with endogenous lipid PI(3,4,5)P<sub>3</sub> (53). This polarization behavior is captured in the models by postulating that the receptor regulates a signal that pushes a downstream subsystem into a parameter regime where the homogeneous state is unstable; thus noise is able to cause a transition from the unstable homogeneous state to a heterogeneous state by means of the Turing instability (33). This mechanism is an instability mechanism that crucially depends on differences in diffusion coefficients of the species involved. In these models, the system at basal state does not have multiple attractors; however, it is easily pushed into a regime of multiple attractors, by varying receptor occupancy, even homogeneously. Most important is the fact that this nonlinear dynamic effect is also utilized in the gradient sensing pathway.

We discuss the possibility of nonlinear effects in the context of one specific kind of intrinsic polarity process: that occurring during *Dictyostelium* development. The basal state of these cells is not stationary: cells 4 h into development are weakly polarized at best (in its early stages of intrinsic polarization), but are still moving by extending pseudopods in random directions (5). When these cells are stimulated by a homogeneous signal, they exhibit a transient (so-called cringe) response; however, they do not become strongly (and persistently) polarized with a clear, sharp, and persistent separation of front and back. Thus, a homogeneous input does not induce the kind of (persistent) polarization that is observed in the course of development. We therefore conclude that the presence of an intrinsic polarization process in *Dictyostelium* such as that in development does not necessarily imply a pattern-forming/instability mechanism involved in the gradient-sensing and polarization pathways. Further, a nonlinear dynamic transition in the polarization pathways would have to be consistent with no signature of such a transition in homogeneous stimulation: we have demonstrated exactly how such a scenario can occur.

## Pattern-forming mechanisms and intrinsic polarity

Regarding the intrinsic polarity process itself, inhomogeneous polarity cues must first be created, which itself would need some kind of symmetry-breaking/pattern-forming mechanism. We have avoided formulating a specific model to describe this. It is possible to employ a mechanism similar to that of Narang (32) to lead to the formation of frontness and backness profiles, with the difference that the signal pushing the system into a pattern-forming regime is an intrinsic signal, and is not necessarily related to receptor pathways. Purely intrinsic processes would lead to the formation of polarity cues, which then regulate various components of the chemotactic pathways. More generally, from our analysis in this article, we see that it is entirely possible that the symmetry-breaking mechanism responsible for generation of polarity cues is not employed by the chemotactic pathways.

Finally, we briefly address a related question: given the above evidence, is it possible that the intrinsic polarity cue generation pattern-forming process is actually employed/controlled by receptor-mediated pathways? As we have discussed before, this is certainly not necessary. However, it is not ruled out either. The analysis of a different mechanism of the activator-inhibitor type similar to Subramanian and Narang (10) with the important difference that the critical parameter is regulated by the receptor via local and global pathways shows that it is possible for a nonlinear pattern-forming mechanism to be responsible for the generation of intrinsic cues. Because of the nature of the receptor regulation, homogeneous stimulation would cause adaptation, and the behavior in a gradient would employ in a heterogeneous fashion, i.e., a nonlinear transition. In this case, there would be a pattern-forming mechanism employed by both intrinsic pathways, and the receptor controlled pathways, without any nonlinear transition in homogeneous stimulation. This kind of mechanism would be somewhat similar to the mechanisms of the literature (10,32) except that the critical parameter is regulated by the receptor by a combination of local and global pathways, leading to adaptation in homogeneous stimulation. This would imply a nonlinear transition early in the receptor-controlled polarization pathways; however, we know of no evidence for this effect.

We thank members of the Iglesias lab and Peter Devreotes for various useful discussions during the course of this work.

We also gratefully acknowledge financial support from the National Science Foundation (grant No. DMS-083500) and the National Institutes of Health (grant No. 71920).

## REFERENCES

1. Haugh, J. M., F. Codazzi, M. Teruel, and T. Meyer. 2000. Spatial sensing in fibroblasts mediated by 3' phosphoinositides. *J. Cell Biol.* 151:1269–1280.
2. Servant, G., O. D. Weiner, P. Herzmark, T. Balla, J. W. Sedat, and H. R. Bourne. 2000. Polarization of chemoattractant receptor signaling during neutrophil chemotaxis. *Science*. 287:1037–1040.
3. Parent, C. A., and P. N. Devreotes. 1999. A cell's sense of direction. *Science*. 284:765–770.
4. Iglesias, P. A., and A. Levchenko. 2002. Modeling the cell's guidance system. *Sci. STKE*. 2002:RE12.
5. Devreotes, P., and C. Janetopoulos. 2003. Eukaryotic chemotaxis: distinctions between directional sensing and polarization. *J. Biol. Chem.* 278:20445–20448.
6. Rappel, W.-J., P. J. Thomas, W. F. Loomis, and H. Levine. 2002. Establishing direction during chemotaxis in eukaryotic cells. *Biophys. J.* 83:1361–1367.
7. Skupsky, R., W. Losert, and R. J. Nossal. 2005. Distinguishing modes of eukaryotic gradient sensing nematode sperm cells. *Biophys. J.* 89:2806–2824.
8. Postma, M., and P. J. Van Haastert. 2001. A diffusion-translocation model for gradient sensing by chemotactic cells. *Biophys. J.* 81:1314–1323.
9. Narang, A., K. K. Subramanian, and D. A. Lauffenburger. 2001. A mathematical model for chemoattractant gradient sensing based on receptor-regulated membrane phospholipid signaling dynamics. *Ann. Biomed. Eng.* 29:677–691.
10. Subramanian, K. K., and A. Narang. 2004. A mechanistic model for eukaryotic gradient sensing: spontaneous and induced phosphoinositide polarization. *J. Theor. Biol.* 231:49–67.
11. Parent, C. A., B. J. Blacklock, W. M. Froehlich, D. B. Murphy, and P. N. Devreotes. 1998. G protein signaling events are activated at the leading edge of chemotactic cells. *Cell*. 95:81–91.
12. Janetopoulos, C., L. Ma, P. N. Devreotes, and P. A. Iglesias. 2004. Chemoattractant-induced phosphatidylinositol 3,4,5-trisphosphate accumulation is spatially amplified and adapts, independent of the actin cytoskeleton. *Proc. Natl. Acad. Sci. USA*. 101:8951–8956.
13. Krishnan, J., and P. A. Iglesias. 2004. A modeling framework describing the enzyme regulation of membrane lipids underlying gradient perception in *Dictyostelium* cells. *J. Theor. Biol.* 229:85–99.
14. Ma, L., C. Janetopoulos, L. Yang, P. N. Devreotes, and P. A. Iglesias. 2004. Two complementary, local excitation, global inhibition mechanisms acting in parallel can explain the chemoattractant-induced regulation of PI(3,4,5)P<sub>3</sub> response in *Dictyostelium* cells. *Biophys. J.* 87:3764–3774.
15. Arriuerlou, C., and T. Meyer. 2005. A local coupling model and compass parameter for eukaryotic chemotaxis. *Dev. Cell*. 8:215–227.
16. Lauffenburger, D. A., and A. F. Horwitz. 1996. Cell migration: a physically integrated molecular process. *Cell*. 84:359–369.
17. Drubin, D. G., editor. 2000. *Cell Polarity*. Oxford Press, London.
18. Nelson, W. J. 2003. Adaptation of core mechanisms to generate cell polarity. *Nature*. 422:766–774.
19. Wedlich-Soldner, R., and R. Li. 2003. Spontaneous cell polarization: undermining determinism. *Nat. Cell Biol.* 5:267–270.
20. Sohrmann, M., and M. Peter. 2003. Polarizing without a cue. *Trends Cell Biol.* 13:526–533.
21. Kimmel, A. R., and R. A. Firtel. 2004. Breaking symmetries: regulation of *Dictyostelium* development through chemoattractant and morphogen signal-response. *Curr. Opin. Genet. Dev.* 14:540–549.
22. Van Haastert, P. J. M., and P. N. Devreotes. 2004. Chemotaxis: signaling the way forward. *Nat. Rev. Mol. Cell Biol.* 5:626–634.
23. Manahan, C. L., P. A. Iglesias, Y. Long, and P. N. Devreotes. 2004. Chemoattractant signaling in *Dictyostelium*. *Annu. Rev. Cell Dev. Biol.* 20:223–253.
24. Servant, G., O. D. Weiner, E. R. Neptune, J. W. Sedat, and H. R. Bourne. 1999. Dynamics of a chemoattractant receptor in living neutrophils during chemotaxis. *Mol. Biol. Cell*. 10:1163–1178.
25. Jin, T., N. Zhang, Y. Long, C. A. Parent, and P. N. Devreotes. 2000. Localization of the G protein  $\beta\gamma$  complex in living cells during chemotaxis. *Science*. 287:1034–1036.
26. Chung, C. Y., S. Funamoto, and R. A. Firtel. 2001. Signaling pathways controlling cell polarity and chemotaxis. *Trends Biochem. Sci.* 26:557–566.
27. Iijima, M., and P. Devreotes. 2002. Tumor suppressor PTEN mediates sensing of chemoattractant gradients. *Cell*. 109:599–610.
28. Funamoto, S., R. Meili, S. Lee, L. Parry, and R. A. Firtel. 2002. Spatial and temporal regulation of 3-phosphoinositides by PI 3-kinase and PTEN mediates chemotaxis. *Cell*. 109:611–623.
29. Krishnan, J., and P. A. Iglesias. 2005. A modeling framework describing the enzyme regulation of membrane lipids underlying gradient perception in *Dictyostelium* cells. II: Input-output analysis. *J. Theor. Biol.* 235:504–520.
30. Levchenko, A., and P. A. Iglesias. 2002. Models of eukaryotic gradient sensing: application to chemotaxis of amoebae and neutrophils. *Biophys. J.* 82:50–63.
31. Wolpert, L. 2002. *Principles of Development*. Oxford Press, London.
32. Narang, A. 2006. Spontaneous polarization in eukaryotic gradient sensing: a mathematical model based on mutual inhibition of frontness and backness pathways. *J. Theor. Biol.* 240:538–553.

33. Gamba, A., A. de Candia, S. Di Talia, A. Coniglio, F. Bussolino, and G. Serini. 2005. Diffusion-limited phase separation in eukaryotic chemotaxis. *Proc. Natl. Acad. Sci. USA*. 102:16927–16932.
34. Levine, H., and W.-J. Rappel. 2005. Membrane-bound Turing patterns. *Phys. Rev. E Stat. Nonlin. Soft Matter Phys.* 72:061912.
35. Maree, A., A. Jilkine, A. Dawes, V. Grieneisen, and L. Edelstein-Keshet. 2006. Polarization and movement of keratocytes: a multiscale modeling approach. *Bull. Math. Biol.* 68:1169–1211.
36. Chen, L., C. Janetopoulos, Y. E. Huang, M. Iijima, J. Borleis, and P. N. Devreotes. 2003. Two phases of actin polymerization display different dependencies on PI3,4,5P<sub>3</sub> accumulation and have unique roles during chemotaxis. *Mol. Biol. Cell.* 14:5028–5037.
37. Albrecht, E., and H. R. Petty. 1998. Cellular memory: neutrophil orientation reverses during temporally decreasing chemoattractant concentrations. *Proc. Natl. Acad. Sci. USA*. 95:5039–5044.
38. Devreotes, P. N., and S. H. Zigmond. 1988. Chemotaxis in eukaryotic cells: a focus on leukocytes and *Dictyostelium*. *Annu. Rev. Cell Biol.* 4:649–686.
39. Krishnan, J., and P. A. Iglesias. 2003. Analysis of the signal transduction properties of a module of spatial sensing in eukaryotic chemotaxis. *Bull. Math. Biol.* 65:95–128.
40. Wang, F., P. Herzmark, O. D. Weiner, S. Srinivasan, G. Servant, and H. R. Bourne. 2002. Lipid products of PI(3)Ks maintain persistent cell polarity and directed motility in neutrophils. *Nat. Cell Biol.* 4: 513–518.
41. Pirone, D. M., and C. S. Chen. 2004. Strategies for engineering the adhesive microenvironment. *J. Mammary Gland Biol. Neoplasia*. 9:405–417.
42. Xu, J., F. Wang, A. Van Keymeulen, P. Herzmark, A. Straight, K. Kelly, Y. Takuwa, N. Sugimoto, T. Mitchison, and H. R. Bourne. 2003. Divergent signals and cytoskeletal assemblies regulate self-organizing polarity in neutrophils. *Cell*. 114:201–214.
43. Postma, M., L. Bosgraaf, H. M. Loovers, and P. J. Van Haastert. 2004. Chemotaxis: signaling modules join hands at front and tail. *EMBO Rep.* 5:35–40.
44. Ridley, A., M. Schwartz, K. Burridge, R. Firtel, M. Ginsberg, G. Borisy, J. Parsons, and A. Horwitz. 2003. Cell migration: integrating signals from front to back. *Science*. 302:1704–1709.
45. Williams, H. P., and A. J. Harwood. 2003. Cell polarity and *Dictyostelium* development. *Curr. Opin. Microbiol.* 6:621–627.
46. Gracheva, M. E., and H. G. Othmer. 2004. A continuum model of motility in amoeboid cells. *Bull. Math. Biol.* 66:167–193.
47. Mogilner, A., and D. Verzi. 2003. A simple 1-D physical model for the crawling of nematode sperm cells. *J. Stat. Phys.* 110:1169–1189.
48. Li Jeon, N., H. Baskaran, S. K. W. Dertinger, G. M. Whitesides, L. Van de Water, and M. Toner. 2002. Neutrophil chemotaxis in linear and complex gradients of interleukin-8 formed in a microfabricated device. *Nat. Biotechnol.* 20:826–830.
49. Song, L., S. M. Nadkarni, H. U. Bodeker, C. Beta, A. Bae, C. Franck, W. J. Rappel, W. F. Loomis, and E. Bodenschatz. 2006. *Dictyostelium discoideum* chemotaxis: threshold for directed motion. *Eur. J. Cell Biol.* In press.
50. Vicker, M. G. 2002. Eukaryotic cell locomotion depends on the propagation of self-organized reaction-diffusion waves and oscillations of actin filament assembly. *Exp. Cell Res.* 275:54–66.
51. Postma, M., J. Roelofs, J. Goedhart, T. W. J. Gadella, A. J. W. G. Visser, and P. J. M. Van Haastert. 2003. Uniform cAMP stimulation of *Dictyostelium* cells induces localized patches of signal transduction and pseudopodia. *Mol. Biol. Cell.* 14:5019–5027.
52. Mikhailov, A. S. 1996. Foundations of Synergetics. Springer, Berlin.
53. Niggli, V. 2000. A membrane-permeant ester of phosphatidylinositol 3,4,5-trisphosphate (PIP<sub>3</sub>) is an activator of human neutrophil migration. *FEBS Lett.* 473:217–221.